TRANSEQUATORIAL LOOPS INTERCONNECTING McMATH REGIONS 12472 AND 12474

Z. ŠVESTKA, A. S. KRIEGER, and R. C. CHASE
American Science and Engineering, Inc., Cambridge, Mass., U.S.A.

and

R. HOWARD
Hale Observatories, Carnegie Institution of Washington, California Institute of Technology, Pasadena, Calif., U.S.A.

(Received 2 March; in revised form 30 April, 1976)

Abstract. We discuss the life-story of a transequatorial loop system which interconnected the newly born active region McMath 12474 with the old region 12472. The loop system was probably born through reconnection accomplished 1.5 to 5 days after the birth of 12474 and the loops were observed in soft X-rays for at least 1.5 days. Transient 'sharpenings' of the interconnection and a striking brightening of the whole loop system for about 6 hr appear to be caused by magnetic field variations in the region 12474. A flare might have been related to the brightening, but only in an indirect way: the same emerging flux could have triggered the flare and at the same time strengthened the magnetic field at the foot-points of the loops. Electron temperature in the loop system, equal to 2.1×10^6 K in its quiet phase, increased to 3.1×10^6 K during the brightening. Electron density in the loop system was $\leq1.3\times10^9$ cm^{-3} and it could be estimated to $\sim7\times10^8$ cm^{-3} prior to the brightening. During the brightening the loops became twisted. There was no obvious effect whatsoever of the activity in 12474 upon the in erconnected old region. The final decay of the loop system reflected the decay of magnetic field in the region 12474.

1. Introduction

Soft X-ray photographs made by the AS & E S-054 experiment during the Skylab mission (Vaiana *et al.*, 1974) have revealed the existence of many loops interconnecting separate active regions on the Sun. In a preliminary study, Chase *et al.* (1975) could detect about one hundred such loops and more than 20 of them were crossing the equator.

In the present paper, we have selected one of these transequatorial loops for a detailed study. This particular loop has been selected because we could follow its complete life-story on the Sun and because, during its life, it has demonstrated several transient phenomena which appear to characterize this type of loop connection on the Sun.

2. Birth of the Loop

The selected loop connected the active regions with McMath plage numbers 12472 and 12474. The region 472 was born one rotation before, on July 11, 10° south of the equator. When it appeared again on the eastern limb on July 30 (Figure 1), it showed pronounced loop structure, but no loops were extending

Solar Physics **52** (1977) 69–90.

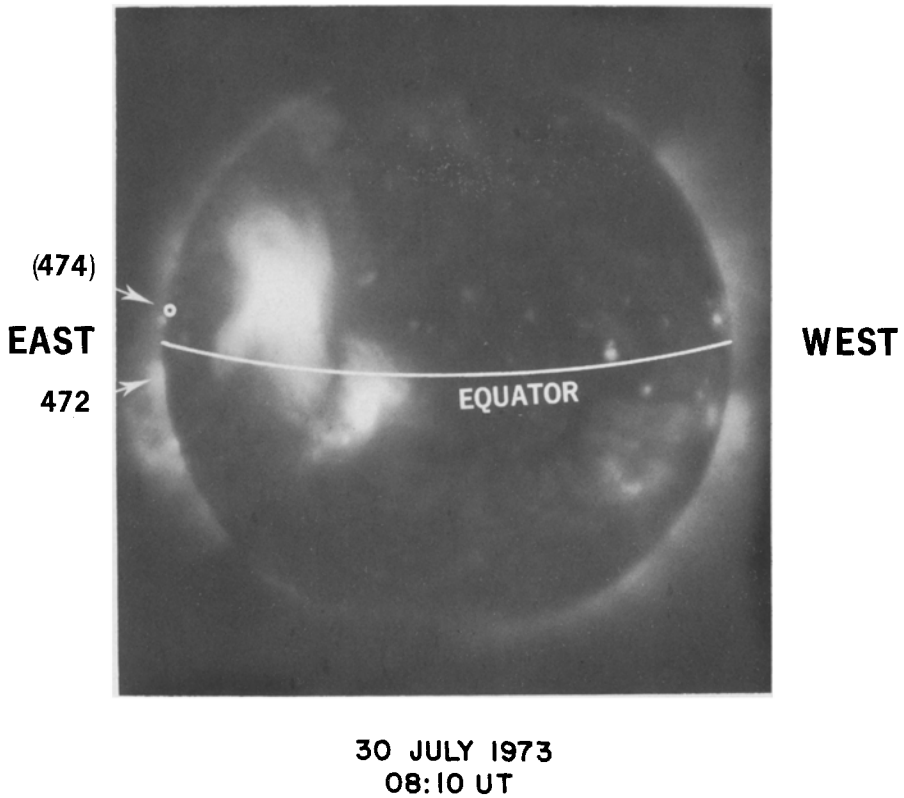

Fig. 1. Soft X-ray photograph of the Sun on 30 July, 1972. Loops of the region McMath 12472 are visible on the eastern limb, but no loop connection can be seen across the equator to the place (marked with a circle) where the region 12474 was born three days later.

towards, or across, the equator. The region 474 did not exist yet at this time. It was born, in the position shown on the figure, at 7° north, only three days later, between 14 and 18 hr on August 2. Figure 2a demonstrates this birth, and one can see that there was no indication of any interconnection between these two regions on August 2 and 3. On August 4, however (the first picture in Figure 2b), the young region began to form a loop-like extension in the direction where later on the interconnecting loop became visible. Unfortunately, there was a break in Skylab photographs from August 4 afternoon to August 6 morning (in UT time), due to crew exchange. On August 6 the interconnecting loop is already clearly indicated and it became very distinct in the morning hours of August 7 (Figure 2b).

This does not seem to be the most common way of birth of an interconnecting loop. More often (as far as we can judge from our material) the interconnecting loops are not newly born magnetic interconnections. The magnetic field lines exist before and become visible in X-rays within a short time after a new active region has emerged near their feet. An example of this is the interconnection born on 5/6 July illustrated schematically in the left part of Figure 3. But this obviously

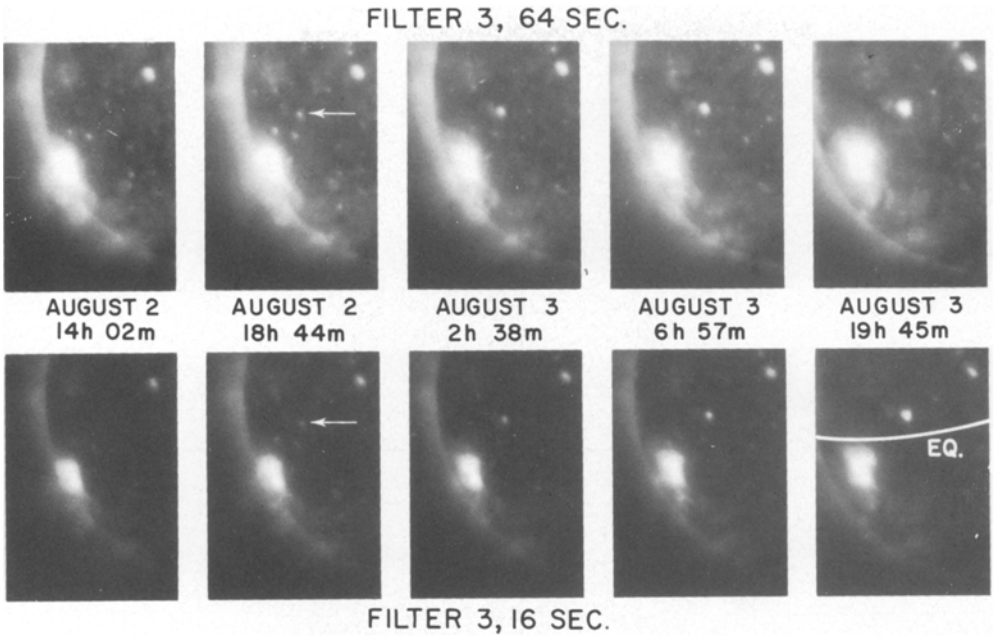

Fig. 2a. Birth of the active region McMath 12474 on August 2 (arrow). Bandwidth of filter 3: 2-32 Å and 44-54 Å. In all figures (except Figure 3) west is to the right.

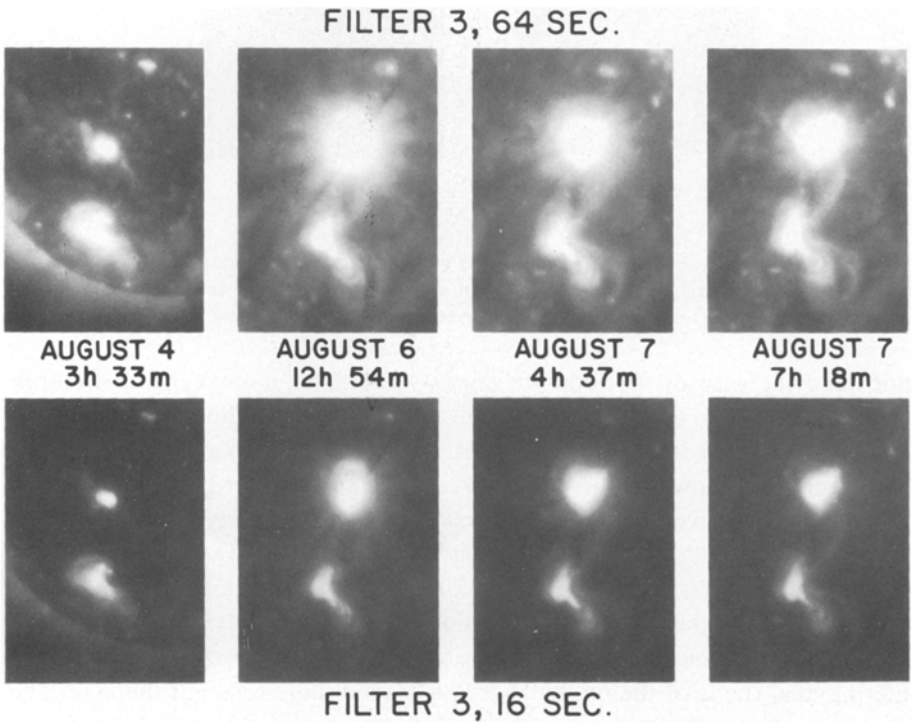

Fig. 2b. Birth of the interconnecting loop between the old region McMath 12472 (below) and the newly born one, McMath 12474 (above).

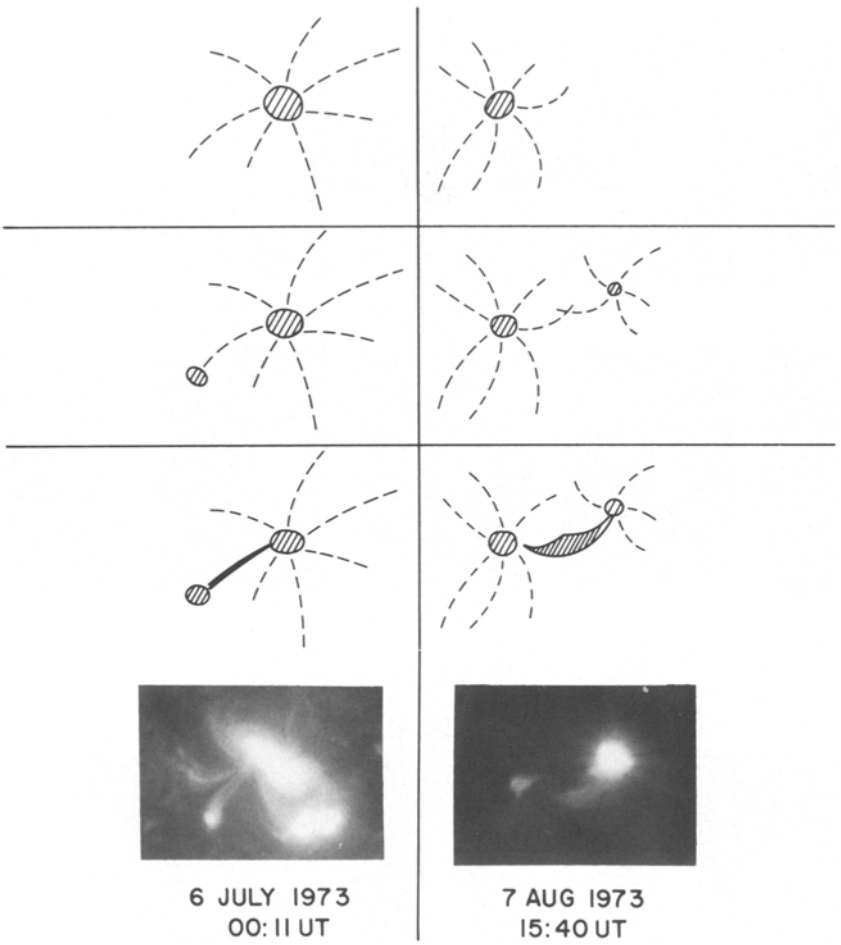

Fig. 3. Schematic drawings of two different ways in which interconnecting loops appear to be born: (a) By making a pre-existing magnetic connection visible in X-rays (on the left); (b) Through reconnection (on the right). Photographs below demonstrate examples of these two modes of birth.

has not been the case of the loop we discuss here. This loop seems to be born through reconnection of two systems of field lines extending from the two different active regions towards each other: an old magnetic structure extending from the region 472 towards the equator reconnected with newly formed magnetic field lines progressively extending southwards from the newly emerging region 474. The right-hand side of Figure 3 demonstrates schematically this type of birth.

There are three facts that substantiate this model. First, as Figures 1 and 2a clearly demonstrate, there was no indication of a loop connection between the two regions prior to and during the first two days of existence of the region 474; second, the final shape of the interconnection has a double-crescent shape (cf. the last drawing and the photograph in the lower right corner of Figure 3, as well as Figure 7) with a 'nose' pointed to the photosphere, which indeed can be explained

most easily through a reconnection of two loops originally rooted near the equator between the two active regions; as we shall see in Section 5.3, there are loops of opposite magnetic orientation, which did not reconnect and are rooted where the 'nose' is seen; and third, as Chase *et al.* (1975) have shown, the transequatorial loops are in general about twice as long as the one-hemisphere loops. This would be the case if all (or most) one-hemisphere loops are born in the way demonstrated at the left-hand side of Figure 3, while all (or most) transequatorial loops are born through reconnection of two loops.

The unfortunate break in Skylab work on August 5 did not give us any opportunity to see the actual reconnection. It certainly did not occur before 03^h on August 4 and it might have been accomplished prior to 13^h on August 6 (but we still may encounter two unconnected loops at that time); definitely, the reconnection did exist at 14^h on August 7 when the whole loop (i.e., both its hypothetical components) brightened (cf. Figure 7). Thus, the reconnection process took more than 33 hr, possibly less than 95 hr, and definitely less than 120 hr, starting from the time when the new flux (i.e., region 474) emerged.

3. The Interconnected Active Regions

The region 472 was a typical old active region with one big remaining spot of the preceding (northern) magnetic polarity. The region was purely bipolar, as one can see from Figure 4, with a well-developed extensive system of internal hot X-ray

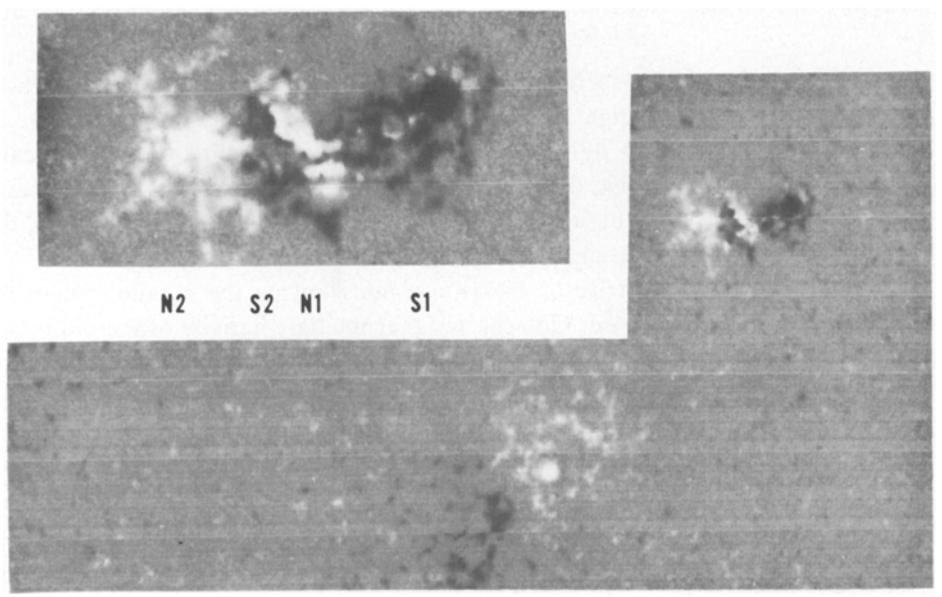

Fig. 4. Kitt Peak magnetogram shows the magnetic configurations of the old region McM 12472 (below) and the newly born McM 12474 (above) at $19^h\,35^m$ UT on August 7. The insert shows the detailed structure of the active region 12474 at $14^h\,45^m$ UT on August 7. The notations Nk, Sk are for reference in the text. (Courtesy of J. W. Harvey, Kitt Peak National Observatory.)

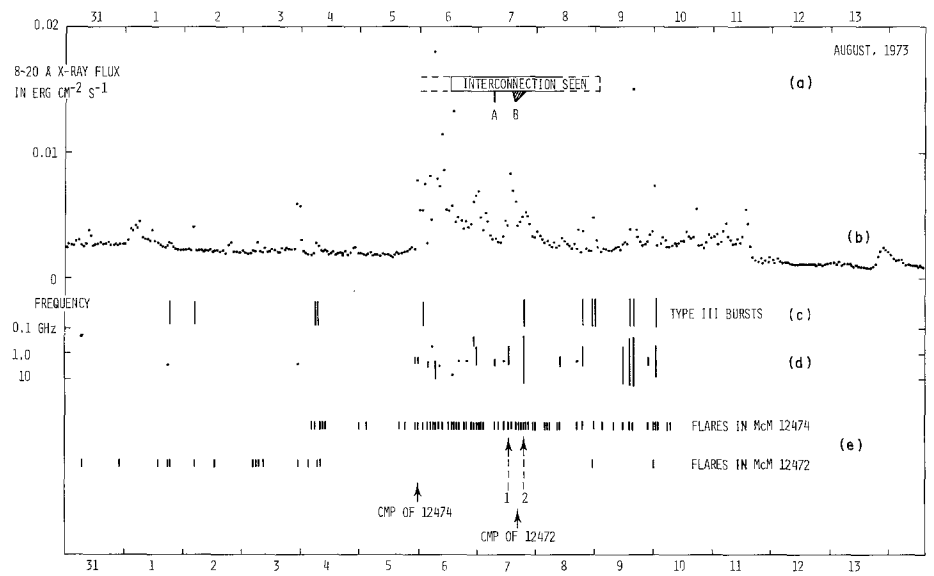

Fig. 5. Scheme of activity in the two interconnected regions. From above: (a) Time period when the interconnecting loop was visible in X-rays. A marks the sharpening and B the brightening of the loop discussed in paragraphs 4 and 5. (b) Hourly flux of 8-20 Å X-rays according to SOLRAD-9 measurements. (c) Type III bursts possibly associated with flares in McM 12472 or 474. (d) Radio bursts at higher frequencies possibly associated with flares in the two studied active regions. (e) Flare (essentially subflare) occurrence in the two active regions. 1 marks the flare which might have been responsible for the brightening B. 2 marks another flare, with outstanding microwave and type III bursts which did not influence the loop-connection at all. (The data (b) to (e) have been taken from *Solar Geophysical Data*, NOAA, Boulder.)

loops (Figures 2b and 7) surrounding a cool quiescent filament, and the whole configuration did not change much during the transit across the solar disk. In contrast, the young region 474 developed very fast and built up a magnetically complex γ-configuration five days after its birth, on August 7. Figure 4 demonstrates the complex magnetic structure in this region on that day. On August 8 the situation began to simplify and the region started to decay (cf. Section 8).

Figure 5 shows the activity of the two regions during the rotation when the interconnection was observed. One can see that the flare activity of the old region 472 decayed on August 4, while on the same day the newly born 474 first started to produce flares. Activity in 474 was much more prominent in microwave and X-ray bursts (as is generally the case in magnetically complex active regions), but it decayed very fast on August 10. The old region 472 produced only two isolated subflares on August 8 and 9 and was also completely inactive from August 10 onwards. (On August 10, region 474 was at ~60° W and 472 at ~40° W on the disk.) However, the internal loop structure in 472 began to change at that time. The final product of these rearrangements was an outstanding loop burst behind the limb on August 13, also detectable in the global soft X-ray flux (cf. the X-ray peak on August 13 in Figure 5). It looked like a loop-prominence system following a large flare, but the complete lack of activity before suggests

that most probably it was a powerful disparition brusque of the quiescent filament, possibly associated with a flare of the "spotless" type described by Dodson and Hedeman (1970).

4. Sharpening of the Loop

As one can see on the last frame of Figure 2b, the interconnecting loop became particularly distinct in the morning hours of August 7. The sharpening of the loop was accomplished between $4^h\,48^m$ and $6^h\,29^m$ UT. The next photograph was taken at $12^h\,08^m$ (the first frame in Figure 7a); the sharp connection became less distinct again, but another bright and sharp loop, with a smaller curvature (thus probably at lower altitude) became visible in addition to the original one.

There was no flare, nor subflare, in any of the regions, between 3^h and $7^h\,30^m$ UT (cf. Figure 5). Hence the effect of sharpening was clearly not flare-associated, and it must have been due to a restructuring of the magnetic field in either of the active regions. Similar 'sharpenings' are occasionally observed in other interconnecting loops as well.

Figure 6 shows the position of the loop in relation to the underlying magnetic field, at $7^h\,17^m$ UT on August 7. In general, one cannot determine with certainty the precise location of the foot points of the interconnecting loops, because they are lost in the bright emission of active regions and, in any case, the X-ray loops cannot be followed to their ends through and below the transition layer. Thus one must extrapolate the curve of the loop towards the expected foot point and this procedure is fairly subjective. In Figure 6 the end of the loop that goes toward

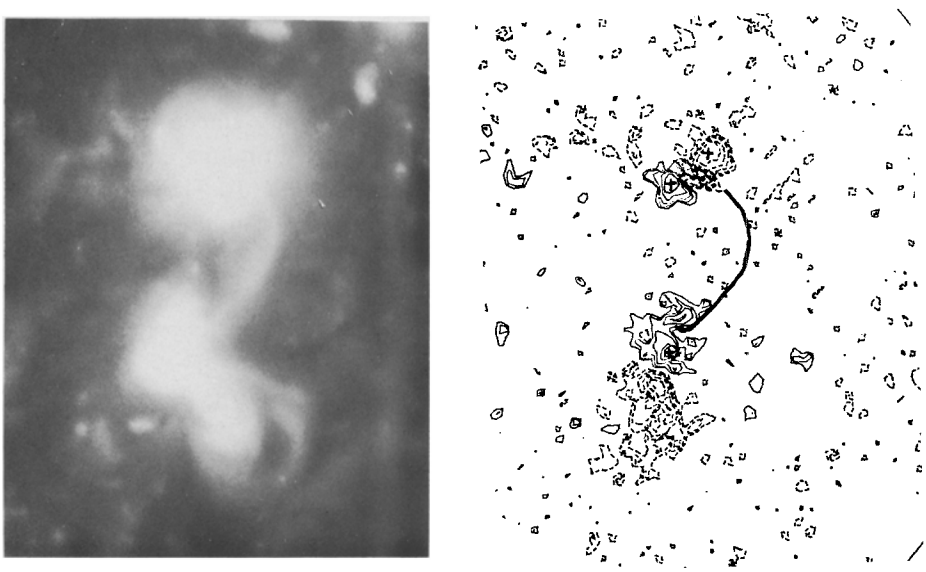

Fig. 6. The interconnecting loop at $7^h\,17^m$ UT on August 7, compared with photospheric magnetic field (Mt. Wilson map; the crosses mark positions of the main spots).

474 appears to head for a location following the main leading spot. The other end of the loop, in 472, heads directly for the large single spot there if one extrapolates the loop in the most straightforward way. However, there are some indications that the loop is significantly curved in its lowest portion and actually heads for the magnetic peak located to the NW of the spot. The indications are as follows:

(a) Careful examination of the X-ray photographs does not exclude the curvature.

(b) In later phases of development (Figure 9a and b) the loops were definitely rooted in the magnetic hill outside the sunspot.

(c) Also a comparison with EUV photographs, which correspond to lower temperatures and thus show the loop extension to lower levels (this comparison has been kindly made by C. C. Cheng) appears to confirm that the loops were rooted in the magnetic hill NW of the spot from 14^h UT onwards. (No earlier EUV photographs were available.)

Therefore, the loop probably connected the spotless magnetic hill of northern polarity in 472 with the southern-polarity field extending to the east of the leading spot in 474. No sunspot was visible in the hill in 472, but a network of small spots existed in the preceding part of 474. While the field in 472 was fairly stationary, the field and sunspot pattern in 474 varied very fast. Therefore, one can suppose that variations in the magnetic field configuration in 474 were the cause of the sharpening of the loop in the morning hours of August 7.

The X-ray flux can be written as

$$F \sim \int f(T_e) n_e^2 \, \mathrm{d}s \simeq f(T_e) n_e^2 s, \tag{1}$$

where the approximation assumes homogeneous plasma of electron temperature T_e, electron density n_e, and linear thickness s. As we shall see in Section 5, the loop electron temperature was close to 2×10^6 K. Thus, since intensity of essentially all X-ray lines peaks at $T_e > 2 \times 10^6$ K, and continuous emission increases with increasing T_e, $f(T_e)$ is an increasing function of T_e. Hence, according to Equation (1), a brightening of a loop can be due to the following alternative (or combined) effects:

(a) Increase in T_e, i.e., inflow of additional energy into the loop.

(b) Increase in n_e, i.e., inflow of additional gas into the loop.

(c) Increase in $n_e^2 s$, through compression of the loop.

(d) Increase in s, e.g., by turning a flat loop such that its edge is towards the observer.

A sharpening of the loop can be explained through any of these effects. Let us make a plausible assumption that the visible diffuse loop is composed of a conglomerate of elementary loops. Then, for example, a compression of any of these elementary loops would produce its brightening: for a loop with circular cross-section a contraction to one half of its original diameter would make the loop 8 times brighter, even if temperature did not increase. Thus the contracted

loop strikingly predominates in the loop brightness and the whole interconnection appears 'sharp'. The reason for the contraction may be a strengthening of the magnetic field at the loop foot. Effects (a) or (b) in any of the elementary loops would cause similar brightness variation. Also a turning of the loop (effect (d)) might explain the sharpening, but there is no obvious indication that the loop did change its orientation during the period we are interested in.

5. Brightening of the Loop

Figure 7a demonstrates a striking brightening of the interconnecting loop system, first seen at $14^h\,02^m$ UT. The intensity variation of the loop (in filter No. 3) is shown in Figure 8. The maximum brightness (7.6 times the pre-increase peak intensity and 12.8 times the total emitted energy) was observed on the frame taken at $15^h\,40^m$ UT. However, due to the large time-intervals between the successive Skylab photographs, the maximum could have been reached any time between $\sim 14^h\,30^m$ and $\sim 16^h\,30^m$. The onset of the brightening occurred between $12^h\,10^m$ and $14^h\,00^m$ and the loop decayed to its pre-increase brightness at about 19–20^h UT.

A comparison of the loop photographs made through filters No. 3 (2–32 Å and 44–54 Å) and No. 1 (2–17 Å) yields pre- and post-increase 'effective' electron temperature $T_e \simeq 2.1 \times 10^6$ K (for an assumed isothermal line of sight). As Figure 8 shows, during the burst T_e increased to $\sim 3.1 \times 10^6$ K. The relatively large errors involved in this determination are due to differences in the amount of scattered light in filters Nos. 1 and 3, and to the strut effect.

5.1. Flare-association of the brightening

As Figure 5 shows, flares (all essentially subflares) occurred very frequently in the region 474 on that particular day. Only two of them, however, appeared to be of greater importance (after *Solar-Geophysical Data*, NOAA, Boulder): flare No. 1 in Figure 5, at $13^h\,07^m$ UT, with Hα maximum at $13^h\,14^m$, Hα importance Sn, and an impulsive microwave burst at $13^h\,09^m$ extending to 2.7 GHz; and flare No. 2 in Figure 5, at $18^h\,37^m$ UT, with Hα maximum at $18^h\,47^m$, Hα importance Sn, a type III burst, and a strong impulsive microwave burst (up to 11 GHz) at $18^h\,44^m$.

The subflare No. 1 (cf. Figure 8) could have been the source of the loop brightening (the next flare, small and without any radio effect, started only after the loop brightening was first seen). However, two facts make this association doubtful. First, the maximum excitation of the loop occurred more than 80 min (and probably as late as 2 or 3 hr) after the impulsive phase of the flare. And second, the flare No. 2, which appeared to be significantly more important than the flare No. 1, did not affect the loop in any apparent way. A comparison of the Boulder, McMath-Hulbert, and Catania photographs of these flares does not show any difference in their positions. The same ribbon that was seen in emission at 13^h also brightened at $18^h\,40^m$, this time accompanied by one more ribbon,

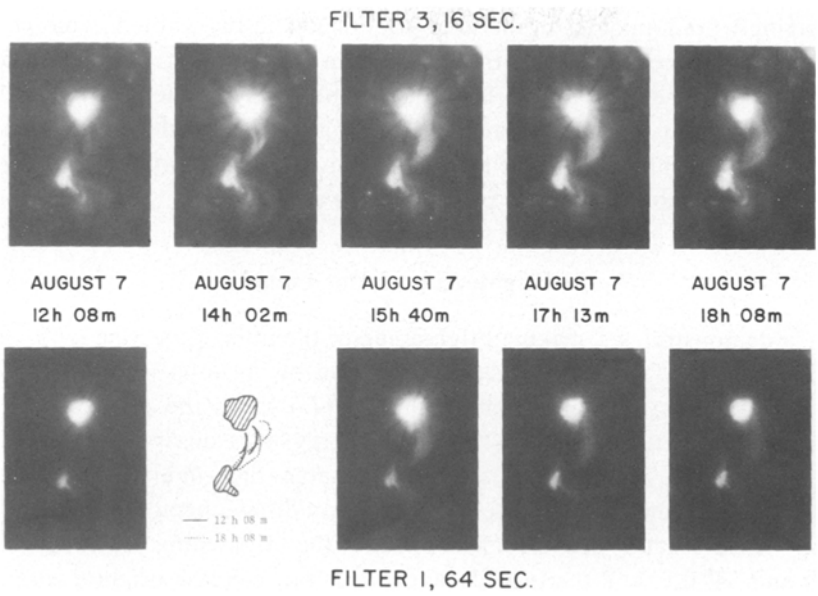

Fig. 7a. Brightening of the interconnecting loops on August 7. Bandwidth of filter 1: 2–17 Å; of filter 3: 2-32 Å and 44-54 Å. The first increase in brightness was seen at $14^h\,02^m$ and maximum brightness was observed at $15^h\,40^m$. The insert shows a schematic drawing of variations in the shape of the loops (by comparing the first and last pictures in this figure).

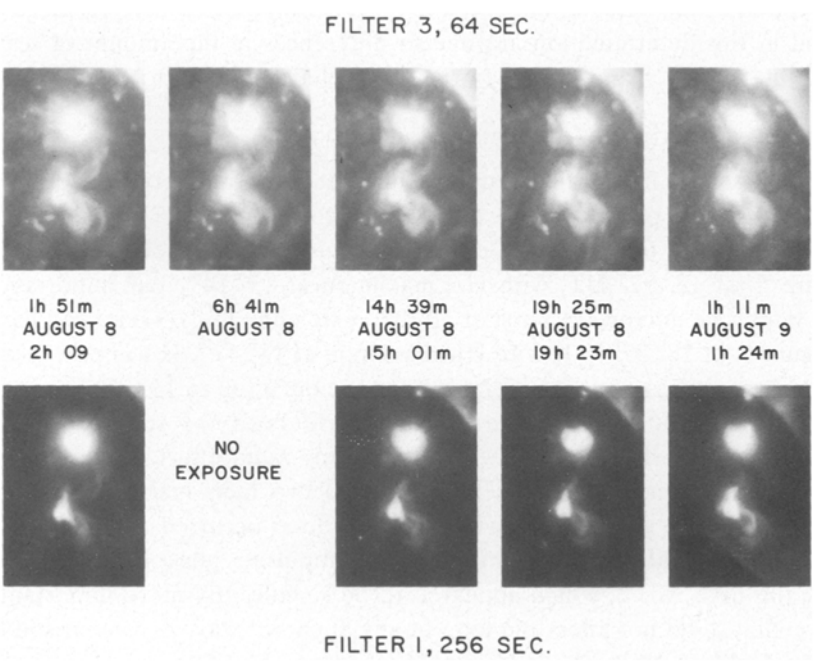

Fig. 7b. The decay phase of the loop connection on August 8/9. Note the twisted shape in the first picture at the left-hand side.

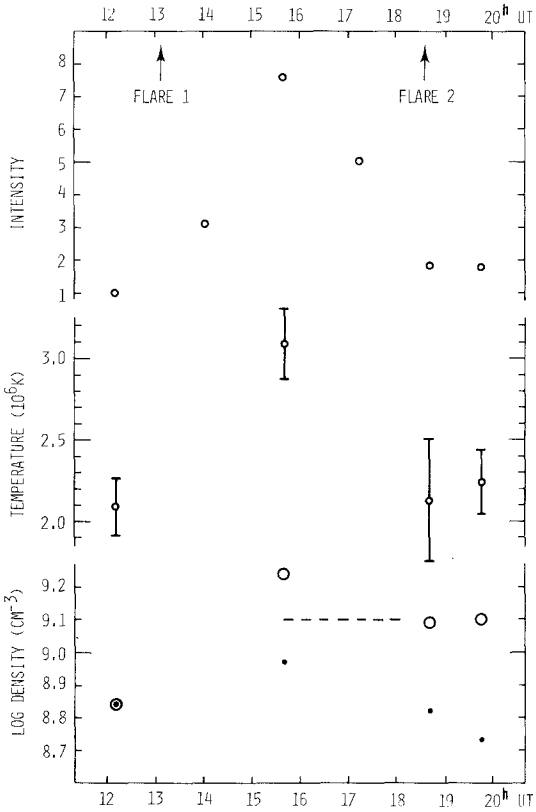

Fig. 8. Photometry of the brightening shown in Figure 7a. From above: (1) Peak intensity in the interconnecting loop, relative to the preincreased brightness at $12^h\,08^m$. (2) Electron temperature (in 10^6 K, with error bars) deduced from filters 1 and 3 (2-17 Å, and 2-32 Å plus 44-54 Å, respectively). (3) Electron density from emission measure, assuming that the loop radial thickness equaled its observed width in the lateral direction at any instant (dots); or, only in the pre-increase situation (at $12^h\,09^m$) being the same at all the other times (circles). The dashed line shows the n_e value corresponding to purely radiative cooling lasting 4 hr (as observed).

thus giving the Hα flare a two-ribbon shape. On SOLRAD, the X-ray burst at $18^h\,40^m$ was at least as intense as at 13^h (no bursts were recorded in between) and the microwave burst at $18^h\,44^m$ had much longer duration and extended to much higher frequencies than that at $13^h\,09^m$.

Therefore, though an association with the flare No. 1 cannot be definitely excluded, one has to take seriously into consideration the possibility that there was no direct association between the loop brightening and the flaring in the region 474. We will discuss both these possibilities more in detail in Section 5.4.

5.2. Cooling of the brightened loop

Figure 8 shows that the excited loop cooled from $T_e \simeq 3.1 \times 10^6$ K to $T_e \simeq 2.1 \times 10^6$ K within approximately 4 hr.

5.2.1. *Radiative Cooling*

Let us assume that the cooling was due solely to radiation. The radiative energy loss per unit volume and second from gas of temperature T_e and density $n_e(=n_i)$ is

$$\frac{\mathrm{d}E}{\mathrm{d}t}=3n_ek\frac{\mathrm{d}T_e}{\mathrm{d}t}=n_e^2p(T_e), \tag{2}$$

where, according to Cox and Tucker (1969), for $10^6<T_e<5\times10^6$ K,

$$p(T_e)\simeq6\times10^{-17}T_e^{-1}. \tag{3}$$

The surplus energy content, $3n_ek(T_{e1}-T_{e2})$, is radiated off after time

$$t_r\simeq3.5n_e^{-1}(T_{e1}^2-T_{e2}^2). \tag{4}$$

Hence, for $T_{e1}=3.1\times10^6$ K and $T_{e2}=2.1\times10^6$ K one finds $n_e\simeq1.3\times10^9$ cm^{-3}.

When knowing T_e, one can also estimate n_e from the emission measure, after making some reasonable assumption about s. By assuming that s is equal to the lateral diameter of the loop at any instant, one gets the n_e values plotted as dots in Figure 8. If, on the other hand, one assumes that s does not change and remains the same as at $12^{\mathrm{h}}\,09^{\mathrm{m}}$ (pre-increase situation), one gets the n_e values plotted as open circles in Figure 8. One can see that the n_e value deduced from t_r under the assumption of purely radiative cooling fits well the electron densities deduced from the emission measure. Thus, the radiative cooling appears to be able to explain fully the decaying phase of the brightening and, in any case, it must have played a significant role in it.

5.2.2. *Loop Inhomogeneities*

There is still another conclusion one can draw from the similarity of the n_e values deduced in the two different ways. Let us suppose that the 'average' n_e value obtained from the emission measure ($\sim10^9$ cm^{-3}) is fictitious, due to the fact that the loop we see is actually composed of many fine loops of x-times higher density. Then, according to Equation (4), the cooling should proceed x-times faster: e.g., for $n_e=10^{10}$ cm^{-3} the cooling time would be 30 min, instead of 4 hr. Thus the four-hours' decay indicates that generally there are no striking inhomogeneities within the loop; as Figure 8 shows, n_e within the emitting region varied no more than about a factor of 2.

Of course, this does not exclude the existence of dense condensations in the maximum phase of the brightening, which might be formed during the heating process, cool faster, rarefy, and eventually merge with the surrounding, less dense loop matter for the definite four-hours cooling. It also does not exclude the existence of loops of slightly different densities and temperatures within the loop system reflecting variations in the magnetic field strength at their foot-points; some of them can be temporarily compressed and heated as we saw in Section 4. However, as soon as this happens, greatly increased radiative cooling tends to

bring these excited loops back to the 'normal' level; so it appears that no striking inhomogeneities can survive for too long.

5.2.3. *Conductive Cooling*

Another mechanism which might contribute to the loop cooling is heat conduction. If we make the assumptions $\nabla T_e \simeq 2T_e/l$ for the temperature gradient, and $V \simeq Al$ for the emitting volume, with A being the cross-section area of the loop and l its length, we can estimate the conductive cooling time by the same method that was applied by Culhane *et al.* (1970) in the case of flare cooling. Spitzer's (1962) coefficient of heat conduction along the field lines, for earlier obtained values of $T_e = 3.1 \times 10^6$ K and $n_3 = 1.3 \times 10^9$ cm^{-3}, is $\kappa = 9.0 \times 10^{-7}\ T_e^{5/2}$. Then the quantity, which Culhane *et al.* called α, equals $17\ l^{-2}$. The distance between the foot-points of the loop was ~24°. Thus $l \simeq 4.5 \times 10^{10}$ cm and the conductive cooling time from $T_e = 3.1 \times 10^6$ K to 2.1×10^6 K should be 3.2 hr, not much different from what we found for the radiative cooling with the same value of $n_e = 1.3 \times 10^9$ cm^{-3}.

Thus the radiation and conduction should both participate in the cooling process of the loop. If $n_e < 1.3 \times 10^9$ cm^{-3}, as it seems to be the case (1.3×10^9 cm^{-3} was the maximum density for pure radiative cooling), the conduction should dominate the cooling. On the other hand, the assumption $V = Al$ may overestimate the conductive loss. Thus it is difficult to say which of these two mechanisms predominates; in any case, however, n_e in the loops must be lower than (but close to) 1.3×10^9 cm^{-3}, and for such values of n_e the loop behavior after the maximum excitation can be well explained by a combination of radiative and conductive cooling.

5.3. Variations in Shape

As one can see in Figure 7a, the loop brightening was accompanied by striking variations in the shape of the interconnecting loops and Figures 9a, b try to relate these shape variations to the underlying magnetic field.

Prior to the brightening, at $12^h\,08^m$, the loop system appears to consist of three loops (Figure 9a, also cf. the first picture and the insert in Figure 7a). One of them (extending more to the west and thus probably higher in the atmosphere) is the original loop of Figure 6, rooted approximately in the same points as before. (Let us call it loop L1). Another loop (L2) is rooted in the same point in 472, but it extends more to the east (and thus probably lower in the atmosphere). Its foot-point in 474 was located more to the east, possibly even in the part marked S2 in Figure 4. Indeed, later photographs indicate that L1 and L2 headed for the two different regions of southern polarity in 474 (marked S1 and S2 in Figure 4). Finally, one can also see a shorter loop (L3) which appears to be rooted between the two active regions. Its foot-point there can be identified with a small negative magnetic feature situated 5° to the west and 2° to the north from the positive magnetic peak in 472 in which the other two loops were most probably rooted.

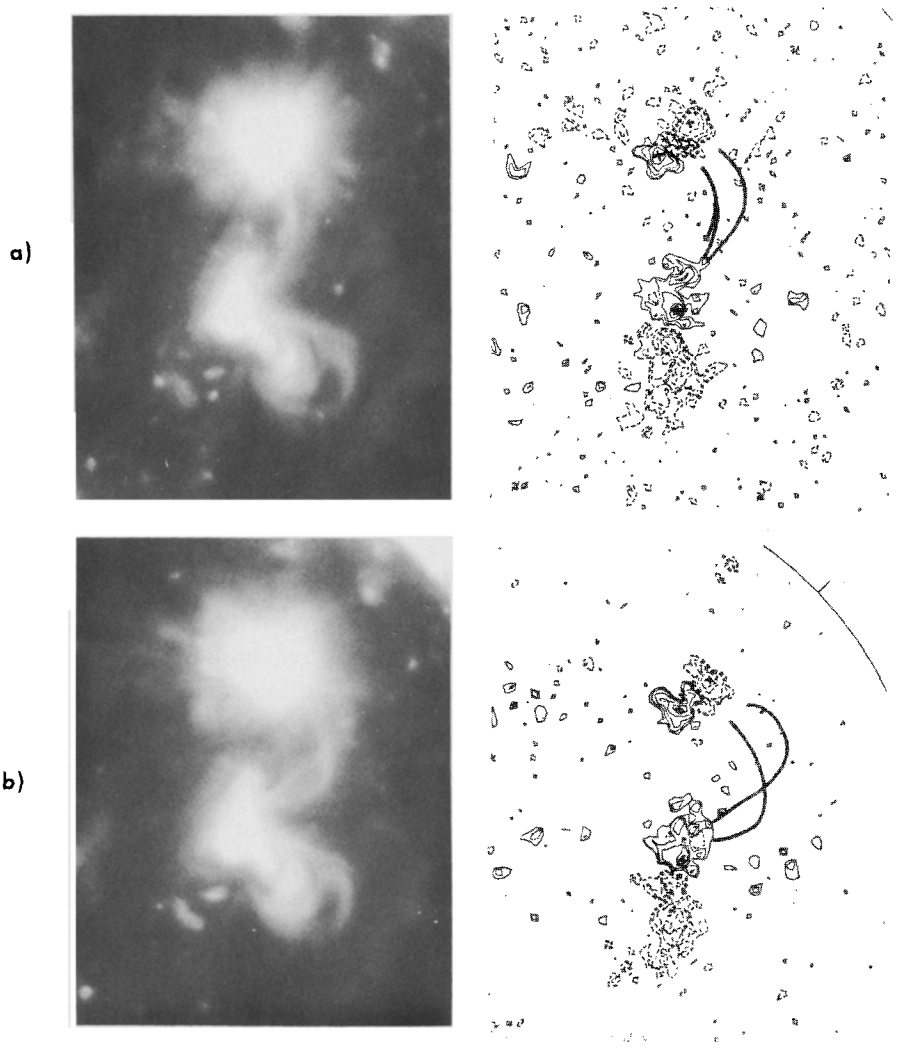

Fig. 9. The interconnecting loops compared with photospheric magnetic field (Mt. Wilson maps; the crosses mark positions of the main spots). (a) X-ray picture and projection on the magnetic map of August 7 at $12^h\,08^m$ UT on August 7; (b) X-ray picture and projection on the magnetic map of August 8 at $01^h\,50^m$ UT on August 8.

Since this foot-point has negative polarity, the loop must be rooted in N1 in 474.

One can consider the short loop a visible remnant of the loop system which extended from 474 southwards prior to the reconnection. Due to the fact that in 472 only the positive magnetic polarity was close to the equator, there were many field lines available for reconnection with field lines coming from both S1 and S2 in 474, but none for reconnecting with field lines coming from N1.

In the early phase of the brightening, at $14^h\,02^m$ UT, both L1 and L2 appear to be heading definitely too far north in 472 to connect with its spot. In 474 the

foot-point of L1 moved more to the east and L2 appears to be rooted in the part S2, as we mentioned above. At $15^h\,40^m$, when the maximum brightness was recorded, the loops became more diffuse, probably due to transient visibility of other elementary loops in the system. Still the interconnection kept its characteristic shape: a narrow cone base in 472, heading for the isolated magnetic peak of preceding polarity there, and a broad base in 474, with foot-points spread in the eastern part of S1 and in S2, according to the notation of Figure 4. One can see very well now the 'nose' pointing eastward (i.e., downwards) towards the negative polarity feature between the two active regions demonstrated in Figure 3, probably the reconnection remnant (Figure 7a, third frame).

During the brightening the loops L1 and L2 expanded to the west (i.e., upwards) and the loop L2 (or a component of it) became greatly twisted. The situation at $1^h\,59^m$ UT on August 8 (corresponding to the first photograph in Figure 7b) is shown in Figure 9b. The rise of the loops can be interpreted as their response to the heating; their expansion can explain the decrease in electron density as compared with the pre-increase state, indicated by the dots in Figure 8. On the other hand, the twist is obviously due to motions of the foot-points in region 474. While the foot-point in 472 is unchanged, the root of L1 moved closer to the leading spot, and the southern polarity S2, in which the loop L2 was rooted, was 'squeezed' south between August 7 and 8. Thus the negative magnetic field traveled much closer to the equator and as the foot-point of L2 was moving along with the magnetic feature, the loop became twisted. These motions of magnetic features need not necessarily be related to the brightening; just a combination of these motions with the loop expansion (caused by the brightening and heating) might have produced the twist.

5.4. Source of the Brightening

Let us first assume that the flare No. 1 at $13^h\,07^m$ UT (cf. Figures 5 and 8) was the source of the brightening. In that case we can see three ways in which the flare could have influenced the loop:

(1) Through heat conduction;
(2) through injection of accelerated particles into the loop;
(3) through evaporation of the flaring chromosphere into the loop.

5.4.1. *Heat Conduction and Gas Evaporation*

Let us suppose that the flare occurred at the place where the loop was rooted so that T_e increased to about 10^7 K near the foot-point of the loop in region 474. Then heat might have been conducted along the magnetic field lines into the loop, in which the pre-increase $T_e \simeq 2\times 10^6$ K.

However, conduction is effective only when the mean free path of the conducting particles is short compared to the extension of the thermal gradient region. For $T_e = 10^7$ K Culhane *et al.* (1970) give 2×10^9 cm^{-3} as the minimum density of ambient plasma in which conduction can occur. The density we deduced earlier is

slightly below this limit which makes the effectiveness of heat conduction questionable. More likely, one would expect in this case a bulk movement of hot plasma which changes our case (1) into case (3): gas evaporation into the loop. Heat conduction downwards can evaporate even chromospheric gas into the loop (Hirayama and Endler, 1975) and the same effect can be expected from streams of energetic electrons which produced the microwave burst (Hudson, 1973; Sturrock, 1973).

However, all these kinds of energetic input are very short-lived. The flare flash phase was finished at $13^h\,14^m$ and lasted only for about 7 min; the impulsive microwave burst occurred at $13^h\,09^m$ and lasted only one minute. The whole flare disappeared at about $13^h\,35^m$ both in Hα light and in soft X-rays (after *Solar-Geophysical Data*, NOAA Boulder). Still, the maximum brightness in the loop was observed as late as at $15^h\,45^m$ and it hardly could occur earlier than about $14^h\,30^m$ (cf. Figure 8), i.e., more than one hour after all energy input into the loop had ceased.

It is quite difficult to find an interpretation for such a long delay in the maximum excitation of the loop. Temperature in the coronal flare decreases fast to its pre-flare value, faster than the emission measure and radiation flux (cf. e.g., Horan (1971) and Milkey *et al.* (1971)). After that there is no obvious reason why the energy content of the loop should further increase. The only explanation might be that the bulk of hot gas (or evaporated chromosphere) fills in only a part of the loop close to the flare. As it propagates along the loop, it cools through expansion and radiation so that (after T_e becomes much less than 10^7 K, but still higher than 2×10^6) the regular heat conduction sets in. Since $\mathrm{d}E/\mathrm{d}t$ is proportional to ∇T_e, the heating of the remnant of the loop would slow down. Then, while the hot part of the loop near 474 would be cooling further, the brightness of the whole loop would still be increasing. However, a comparison with Figure 7a shows that this is not what has been observed, since the whole loop was bright as early as $14^h\,02^m$, and the loops even seem brighter near their tops than near the region 474.

5.4.2. *Particle Injection*

Explanation through particle injection also encounters serious difficulties. The observed microwave burst gives evidence of non-thermal acceleration of electrons to the range of 100 keV energies. As we know from other cases, the best fit to the energy spectrum of the accelerated electrons is a power law, $\mathrm{d}N(E)/\mathrm{d}E = KE^{-\gamma}$, with mean $\gamma \simeq 3$ (Lin and Hudson, 1973; cf. Švestka, 1976). The number of accelerated electrons with energy in excess of 10 keV in a typical burst is $\sim10^{35}$ (Kane and Anderson, 1970) and these electrons carry energy between 10^{27} and 10^{28} erg.

Let us suppose that these non-thermal electrons are injected into the interconnecting loop at the time of the impulsive burst. Through collisions they gradually

transfer their energy to the ambient thermal electrons and thus increase the electron temperature in the loop. Then, however, we encounter two difficulties.

First, the total energy increase in the loop during its brightening can be estimated to be $3k \times 10^9(n_e) \times 10^6(\Delta T_e) \times 4 \times 10^{10}$ (length) $\times 2 \times 10^{19}$ (cross-section) $\simeq 3 \times 10^{29}$ erg. We see that the energy expected in high-energy (>10 keV) particles is insufficient, by more than one order of magnitude. In order to increase the energy input, we must involve also particles below 10 keV which would then dominate the heating and this inclusion in fact brings us back to the model discussed in Section 5.4.1.

Another difficulty is the long delay in the maximum loop temperature. The rate of the energy transfer through collisions to the ambient electrons is (Kane and Anderson, 1970)

$$\frac{dE}{dt} \simeq 5 \times 10^{-9} n_e E^{-1/2} \text{ keV s}^{-1}. \tag{5}$$

As long as this rate exceeds the radiative and conductive energy losses of the ambient plasma, the loop temperature is rising. Figure 8 shows that this rise time must have been one hour or more after the particle injection and this is incompatible with the fact that the bulk of energy must have been brought into the loop by low-energy electrons. For $n_e = 7 \times 10^8$ cm^{-3} (density in the loop prior to the flare according to Figure 8) the integration of Equation (5) shows that electrons with energy of 10 keV thermalize within 6 seconds and those with 100 keV within 3 min. Only electrons with initial energy in excess of 700 keV are not completely thermalized 60 min after the injection. However, even with unrealistically high $\gamma = 2.5$ in the power law (γ usually steeply increases above ~70 keV) there will be only $\sim 2 \times 10^{32}$ electrons with $E > 700$ keV, carrying energy of about 5×10^{23} erg, only an insignificant fraction of the energy input.

Thus non-thermal electrons obviously cannot be responsible for the heating. One can make the assumption that protons are also accelerated, jointly with electrons, during the impulsive phase. But as long as the protons are accelerated to the same energy and $n_e = n_i$ in the loop, the protons will behave in the same way as we described above for the case of the electrons.

5.4.3. *Non-Flare Effects*

For all these reasons, one has to suspect that the loop brightening is not related to the flare at $13^h\,07^m$ UT at all; or, that the relation may be indirect: for example, a newly emerging magnetic flux triggers the flare and at the same time strengthens the magnetic field near the foot-points of the loop.

In any consideration of this kind we are severely limited by the fact that we still do not know the basic mechanism which makes the coronal loop visible in X-rays. It might be current dissipation, wave dissipation, or any other mechanism which enhances the radiation in the loop (cf. items (a) to (d) in Section 4). In any case, a transient brightening of the existing loop implies, for any of the mechanisms, a rearrangement of the magnetic field at one of the foot-points of the loop.

As an example, we will consider heating of the loop by Alfvén waves. This mode of heating has several attractive features. The waves are generated and get through the photosphere only where magnetic field is strong and it is difficult to dissipate them. However, since they propagate along the magnetic field lines, they can dissipate in a loop configuration if they enter into it from both sides and the two wave trains interact near the top of the loop (Wentzel, 1974). Part of the dissipated energy is transformed into heat and we thus see bright X-ray loops in active regions, wherever they connect regions of strong magnetic flux in the photosphere. On the other hand, we rarely see loops of comparable length which go from the active region outwards, and if so, then only in the soft filter No. 3 (i.e., at lower temperature), since the magnetic flux at the outer end of the loop is weak. Such loops become best visible if the outer field strengthens, and this effect is most striking when a new magnetic flux (active region) emerges at the outer end of the loop, or when the loop reconnects with another one, rooted in another active region. These are the cases when we see the interconnecting loops.

In order to produce a transient brightening in a loop which already emits in X-rays we must increase the energy dissipation. The increased dissipation should start near the top of the loop where the wave trains interact. This actually seems to happen at the beginning of the brightening we discuss, at $14^{h}\,02^{m}$ (Figure 7a). Thus, qualitatively, the Alfvén wave dissipation in closed magnetic arches appears to explain fairly well many of the aspects we have observed.

It is believed that Alfvén waves can be efficiently generated in the convection layer wherever the magnetic field is strengthened and, according to Uchida and Kaburaki (1974), the generated waves can get through the photosphere at any place where the magnetic field exceeds a few tens of gauss. Any strengthening of the field improves the photospheric 'transparency' in Alfvén waves and, below the photosphere, enhances the wave production. Thus, any increase in the magnetic field at the foot of a loop increases the energy input into it.

On the other hand, the efficiency of the transformation into heat depends predominantly on the magnetic field in the coronal loop (i.e., on the ratio between Alfvén velocity and the velocity of sound). According to Wentzel's (1974) estimate, an increase in temperature by ΔT_e above initial temperature T_e needs $B \simeq (\Delta T_e/T_e\tau)^{1/2} \times 10^2$ G, where τ is the wave period (assumed $\lesssim 1$ min). Thus, assuming $\tau = 50$ s, in the case we are interested in one would need $B \simeq 8$ G to make the loop visible (by heating it from 1.6×10^6 to 2.1×10^6 K) and this field should increase to $B \simeq 14$ G in order to heat the preheated loop to 3.1×10^6 K. Correspondingly, the photospheric field should also be increased by about a factor of two.

As far as the total energy is concerned, one needs mean energy flux of about $8 \times 10^{25}\,\epsilon^{-1}$ erg s^{-1} in order to build up 3×10^{29} erg in the loop during one hour (cf. Section 5.4.2). ϵ denotes the efficiency of the wave dissipation. With 2×10^{19} cm^2 being the estimated area of the base of the loop in region 474, one needs mean energy flux of about $4 \times 10^6\,\epsilon^{-1}$ erg cm^{-2} s^{-1}. According to Savage (1969) a

spot umbra emits an Alfvén flux of 2×10^{10} erg cm^{-2} s^{-1} and Piddington (1973) estimates flux in a 300 G-field to be $\sim4\times10^{8}$ erg cm^{-2} s^{-1}. Thus the energy required in our case should be available provided that the field at the loop feet is of the order of 100 G and ϵ is not much less than 10^{-1}.

All these considerations, even when based on rough estimates, show that one might expect a loop brightening similar to that we observed, if the magnetic field at the foot of the loop rapidly increased by about a factor of two. This may happen if a new flux emerges just where the loop is rooted, and the active region 474 indeed showed striking field variations at that time. This interpretation removes one of the most serious problems we encountered before, namely the long delay in the maximum temperature and brightness. The flux emergence would take one or more hours, and all this time the loop would gradually brighten as we actually have observed.

6. Decay of the Loop System

The whole loop system once again became very sharp and distinct at $1^{h}\,15^{m}$ on August 8 (first picture in Figure 7b). After that, however, the system rapidly decayed. By 14 39 UT on August 8 the loop L2 was no longer visible and the original loop L1 disappeared around midnight on the same day. Thus the original loop could be seen in soft X-rays for at least 1.5 days; due to gaps in observation its actual life-time could have been 1.5 to 5 days.

The reason for the decay is quite clear, because it reflected a fast decay of the southern magnetic polarity in region 474. While on August 7 Mt. Wilson observed 17 spots of southern polarity in that group, this number dropped to 4 on August 8 and to only one on August 9. As one can see in Figure 5, the fast decay of the region 474 also resulted in a complete end to the production of flares and radio bursts in the early hours of August 10.

7. Physical Relations between the Interconnected Regions

In spite of the fact that the regions 472 and 474 became interconnected across the equator and stayed so for at least two days, one cannot find any changes in the quiet region 472 which might reflect the flaring activity in 474. As Figures 2 and 7 show, the region 472 remained without any apparent change during the whole period of interconnection, even during the striking brightening of the whole loop system. The only change that occurred in 472 during that time was the occurrence of an active flocculus (Dodson-Prince, 1975), which was first seen at $13^{h}\,48^{m}$ UT and lasted for more than one hour. Since, however, another dark flocculus was seen in 472 at $12^{h}\,59^{m}$ UT, prior to the flare in 474 and before the loop was seen to brighten, this association can easily be a chance coincidence.

Nor were there any sympathetic flares in the interconnected regions. Figure 5 shows this fact very clearly, since actually the whole flare activity in 472 stopped

when the activity in 474 set in. Thus a visible loop connection between two active regions evidently does not necessarily imply that one region can influence the other. It is true that one has to be careful in generalizing this statement, since region 472 might not have been in a metastable state capable of flare production (cf. the sudden end of flaring in Figure 5), and in some other cases, when regions lie close to each other, a sort of 'synchronization' of the subflare activity cannot be excluded (Fritzová-Švestková *et al.*, 1976). Nevertheless, even then the existence and non-existence of a visible connection does not seem to be the decisive factor for the occurrence of 'sympathetic' flares.

8. Conclusions

The following conclusions can be drawn from soft X-ray observations of the transequatorial interconnecting loop we discussed in this paper:

(1) The loop was most probably born through reconnection of magnetic field lines extending from the two active regions towards the equator. The reconnection occurred later than 33 hr after the time when the younger region was born.

(2) The fully developed interconnection was composed of several loops. All interconnecting loops appeared to be rooted in a spotless magnetic hill of preceding northern polarity in the old region McM 12472, but spread over two separate spotty regions of southern polarity in the new, magnetically complex, region McM 12474. Loop connections emerging from the northern polarity in 12474 could not reconnect and remained rooted near the equator.

(3) At about 14^{h} UT on August 7 the loop system brightened strikingly, and the original temperature in the loop, $T_e \simeq 2.1 \times 10^6$ K, increased to $T_e \simeq 3.1 \times 10^6$ K in one to three hours. Also the density might have increased by up to factor 2 from the pre-increase value of $n_e \simeq 7 \times 10^8$ cm^{-3}, but these estimates are model-dependent. The cooling time of $\sim$4 hr shows $n_e \leq 1.3 \times 10^9$ cm^{-3} in the loop system during the decay phase.

(4) The good agreement between the n_e values deduced from the emission measure and from the cooling time, respectively, reveals that density inhomogeneities in the loop system could not exceed a factor of 2 during the decay phase. This does not exclude the existence of short-lived condensations of higher density which can cause fast-decaying brightness fluctuations near the maximum phase or temporary 'sharpening' of the loop such as we observed in the morning hours of August 7.

(5) The loop brightening might have been a consequence of an Sn subflare with an impulsive phase that occurred in McMath 12474 at $13^{h}\,07^{m}$ UT. However, neither heat conduction nor particle injection can explain the long time delay in the maximum brightness of the loop. Therefore, it appears more realistic to suppose that the heating was due to a fast strengthening of the magnetic field at the foot-points of the loop system in the active region McM 12474. If the loop heating is due to a dissipation of Alfvén waves, the field, of the order of 100 G,

should have doubled during the brightening. Also in this case there may be an indirect connection with the preceding subflare, which might have been triggered by the same emerging flux that strengthened the magnetic field.

(6) During the brightening the loops became twisted, and this seems to be a consequence of their rise in the corona, while at the same time they stayed rooted in moving magnetic features in the region 12474.

(7) There was no obvious effect whatsoever of the almost continuous subflare activity in region 12474 upon the interconnected region 12472, which stayed quiet and unchanged all the time. Thus a visible loop connection does not necessarily imply that one active region would influence the other.

(8) The loop system ceased to be visible on August 8, in consequence of the fast decay of the magnetic field in the region McM 12474. Thus the transequatorial loop connection visible in X-rays existed for 1.5 to 5 days.

Acknowledgements

Our thanks are due to Dr H. W. Dodson-Prince at the McMath-Hulbert Observatory in Michigan, Dr G. Godoli at the Catania Observatory in Italy, Dr J. W. Harvey at the Kitt Peak National Observatory in Arizona, and to the WDC-A office in Boulder, Colorado, for making their ground-based observations available to us, and to Dr C. C. Cheng of the Naval Research Laboratory in Washington for helpful consultations. The analyzed soft X-ray photographs were obtained by the AS & E S-054 experiment on Skylab, of which Dr G. Vaiana was the Principal Investigator. This work was supported by NASA under contract NAS8-27758.

References

Chase, R. C., Krieger, A. S., Švestka, Z., and Vaiana, G. S.: 1975, *Space Res.* **16** (in press).
Cox, D. P. and Tucker, W. H.: 1969, *Astrophys. J.* **157,** 1157.
Culhane, J. L., Vesecky, J. F., and Phillips, K. J. H.: 1970, *Solar Phys.* **15,** 394.
Dodson, H. W.: 1975, private communication.
Dodson, H. W. and Hedeman, E. R.: 1970, *Solar Phys.* **13,** 401.
Fritzová-Švestková, L., Chase, R. C., and Švestka, Z.: 1976, *Solar Phys.* **48,** 275.
Hirayama, T. and Endler, F.: 1975, *Bull. Am. Astron. Soc.* **7,** 352 (abstract).
Horan, D. M.: 1971, *Solar Phys.* **21,** 188.
Hudson, H. S.: 1973, in R. Ramaty and R. G. Stone (eds.), *Symposium on High Energy Phenomena on the Sun*, NASA-GSFC Preprint, p. 207.
Kane, S. R. and Anderson, K. A.: 1970, *Astrophys. J.* **162,** 1003.
Lin, R. P. and Hudson, H. S.: 1971, *Solar Phys.* **17,** 412.
Milkey, R. W., Blocker, N. K., Chambers, W. H., Fehlan, P. E., Fuller, J. C., and Kunz, W. E.: 1971, *Solar Phys.* **20,** 400.
Piddington, J. H.: 1973, *Solar Phys.* **33,** 363.
Savage, B. D.: 1969, *Astrophys. J.* **156,** 707.
Spitzer, L.: 1962, *Physics of Fully Ionized Gases*, (2nd edition), Interscience Publ., New York-London.
Sturrock, P. A.: 1973, in R. Ramaty and R. G. Stone (eds.), *Symposium on High Energy Phenomena on the Sun*, NASA-GSFC Preprint, p. 3.
Švestka, Z.: 1976, *Solar Flares*, D. Reidel Publ. Company, Dordrecht, Holland.

Uchida, Y. and Kaburaki, O.: 1974, *Solar Phys.* **35,** 451.
Vaiana, G. S., Krieger, A. S., Petrasso, R., Silk, J. K., and Timothy, A. F.: 1974, in L. Larmore and D. Crawford (eds.), *Instrumentation in Astronomy-II*, Seminar Proceedings, Soc. of Photo-Optical Instrumentation Engineers **44,** 185.
Wentzel, D. G.: 1974, *Solar Phys.* **39,** 129.